APPLICATION OF RANDOM FOREST ALGORITHM FOR ARRHYTHMIA DETECTION BASED ON ELECTROCARDIOGRAM DATA

Fransido Situmorang[1]; David William[1]; Jennifer Patterson[1]; Niki Ardila[1]; Mardi Turnip[1*]

System Information[1]
University Prima Indonesia, Medan, Indonesia[1]
https://unprimdn.ac.id[1]
fransido1908@gmail.com, davidrwill29@gmail.com, qxjejen@gmail.com, nikyardilaa@gmail.com,
marditurnip@unprimdn.ac.id[*]

(*) Corresponding Author
(Responsible for the Quality of Paper Content)

Abstract— Arrhythmia is a common cardiac disorder that requires early detection to prevent serious complications. This study applied the Random Forest algorithm to enhance electrocardiogram (ECG) analysis and enable accurate arrhythmia classification. Unlike prior studies that focused primarily on resting ECG signals, this research incorporated dynamic data collected from 26 participants performing three physical activities for three minutes each, capturing physiological variations across multiple activity states. The Random Forest model was constructed and evaluated using ECG-derived temporal and morphological features to detect potential arrhythmias. Experimental results showed that the model achieved an accuracy of 97.4%, with precision, recall, and F1-score each reaching 98%, and an AUC of 0.97. However, several limitations remain, including the relatively small and homogeneous sample, as well as the short recording duration. Nonetheless, the proposed approach demonstrates strong potential to support early cardiac screening and real-time monitoring, particularly in portable and resource-limited healthcare applications.

Keywords: arrhythmia, electrocardiogram, random forest

Intisari— Aritmia merupakan gangguan jantung yang umum terjadi dan memerlukan deteksi dini untuk mencegah komplikasi serius. Penelitian ini menerapkan algoritma Random Forest untuk meningkatkan analisis sinyal elektrokardiogram (ECG) dan memungkinkan klasifikasi aritmia secara akurat. Berbeda dengan penelitian sebelumnya yang berfokus pada sinyal ECG dalam kondisi istirahat, penelitian ini mengintegrasikan data dinamis yang dikumpulkan dari 26 partisipan yang masing-masing melakukan tiga aktivitas fisik selama tiga menit, sehingga mampu menangkap variasi fisiologis pada berbagai kondisi aktivitas. Model Random Forest dibangun dan dievaluasi menggunakan fitur temporal dan morfologis yang diturunkan dari sinyal ECG untuk mendeteksi potensi aritmia. Hasil eksperimen menunjukkan bahwa model mencapai akurasi sebesar 97.4%, dengan nilai presisi, recall, dan F1-score masing-masing sebesar 98%, serta nilai AUC sebesar 0.97. Namun, beberapa keterbatasan tetap ada, termasuk sampel yang relatif kecil dan homogen, serta durasi perekaman yang singkat. Meskipun demikian, pendekatan yang diusulkan menunjukkan potensi yang kuat untuk mendukung skrining jantung dini dan pemantauan secara waktu nyata, terutama pada aplikasi kesehatan portabel dan di lingkungan dengan sumber daya terbatas.

Keywords: aritmia, elektrokardiogram, random forest.

INTRODUCTION

The heart is a vital organ in the cardiovascular system, responsible for maintaining overall health which early detection of it's abnormalities also essential to prevent cardiovascular diseases [1]. According to the World Health Organization (WHO), cardiovascular disease (CVD) remains the leading cause of mortality worldwide, accounting for approximately 17.9 million deaths in 2021 [2]. In Indonesia, a similar situation was observed, where the prevalence of

diagnosed heart disease among individuals of all ages rose from 1.5% in 2018 to 1.7% in 2021 [3]. Despite its high prevalence, early detection of heart disease is still hindered by the lack of practical, accessible, and adaptive diagnostic tools [4]. In many communities, access to cardiac diagnostic resources is further constrained by economic, educational, infrastructural, and awareness-related factors [5].

Electrocardiography (ECG) is the primary method used to detect heart disease, particularly arrhythmia, due to its ability to record electrical activity of the heart in real-time. However, conventional ECG systems such as the 12-lead ECG and Holter monitors are often limited by their dependence on clinical settings, short monitoring durations, and patient discomfort. These constraints reduce their effectiveness in capturing sporadic or asymptomatic events and limit their applicability for long-term monitoring. To address these limitations, recent technological developments have led to more advanced and user-friendly ECG systems. Contemporary solutions include digital ECG devices, mobile applications, and wearable technologies that enable more accessible and continuous cardiac monitoring. AliveCor, for example, is a mobile application approved by the Food and Drug Administration that allows users to transmit ECG signals via smartphones and stores the data on an online server [6]. Similarly, the Apple Watch has been designed to measure heart rate using embedded sensors, offering a convenient and non-invasive method of cardiac monitoring [7].

While these mobile and wearable technologies provide flexibility and ease of use, their diagnostic performance may be compromised by limitations in signal quality and accuracy. Mobile ECGs have been widely used to monitor various heart problems [8], but they often exhibit inconsistencies when analyzing heart signals. To overcome this, more sophisticated systems such as the Wireless Monitoring Holter have been developed. This device connects to a cloud-based platform and leverages deep learning algorithms for real-time data analysis [9]. The collected ECG signals can be transmitted continuously, even during daily activities or sleep, and analyzed through an application such as Vigo using artificial intelligence (AI). Additionally, studies have explored combining Holter monitoring with continuous photoplethysmography (PPG) signal collection [10]. In such cases, subjects were fitted with a Holter monitor and a Garmin smartwatch for a 24-hour period. These two devices were used together to enhance arrhythmia detection by integrating different signal sources. This approach exemplifies the growing trend toward multimodal monitoring for improved diagnostic accuracy.

Signal noise remains a common challenge in ECG monitoring, particularly in ambulatory settings. Previous research has explored several algorithms to address this problem. For instance, the K-Nearest Neighbors (KNN) method with wavelet scattering coefficients from three-axis accelerometer sensors was able to reduce motion-related artifacts in wearable ECG devices [11], and KNN has also been applied to filter abnormal signals on 12-lead ECGs [12]. Deep learning approaches such as Convolutional Neural Network (CNN) and Bi-directional Gated Recurrent Unit (BiGRU) have been employed to classify heartbeat sounds in elderly individuals [13], while Deep Neural Networks (DNNs) have increasingly been used to detect specific cardiac conditions from ECG data [14]. Other approaches include Complex Support Vector Machine (CSVM) for arrhythmia detection [15], Analysis of Variance (ANOVA) with entropy cross-sampling applied to RR intervals [16], multi-layered Artificial Neural Networks (ANNs) for arrhythmia detection [17], and Naïve Bayes for early identification of heart disease [18].

In previous research, an evaluation was conducted on four classification algorithms for detecting heart disease based on clinical data. The results showed that Random Forest achieved the best performance with an accuracy of 87.2%, precision of 85.9%, recall of 86.4%, F1-score of 86.1%, and ROC-AUC value of 0.90. Meanwhile, the SVM algorithm achieved an accuracy of 85.7%, precision of 84%, recall of 83.5%, F1-score of 83.7%, and ROC-AUC of 0.88. In addition, KNN achieved 81.4% of accuracy, a precision of 79.5%, recall of 80.2%, F1-score of 79.8%, and ROC-AUC of 0.84 [19]. These results shows that method such as Random Forest are not only better in accuracy but also offers greater reliability and consistency with improved robustness against overfitting.

Integrating Random Forest into web-based medical systems has demonstrated practical benefits in the early detection of arrhythmia, which is particularly important considering the high mortality rate associated with arrhythmia in Indonesia [20]. Beyond its theoretical strengths, Random Forest has shown consistent performance in clinical applications. When combined with morphological features extracted from ECG signals, the classification of arrhythmias and other cardiac conditions can be further enhanced [21]. This integration of feature engineering with machine learning contributes to improved diagnostic precision and reliability. Random Forest provides several strengths, including the ability to capture

Accredited Rank 2 (Sinta 2) based on the Decree of the Dirjen Penguatan RisBang Kemenristekdikti
No.225/E/KPT/2022, December 07, 2022. Published by LPPM Universitas Nusa Mandiri

363

complex non-linear relationships, effectively manage missing or imperfect data, and maintain a level of interpretability that is crucial in clinical decision-making, as it allows healthcare professionals to understand the reasoning behind the model's predictions [22].

Despite these advantages, there remain gaps in how Random Forest has been applied in previous studies. Most existing work has evaluated its performance primarily on ECG data recorded under resting or single-condition states, without considering the physiological variations induced by different physical activities. This omission is critical, as physical activity significantly influences ECG signal characteristics and may affect diagnostic outcomes.

To address this gap, the present study investigates the performance of Random Forest in classifying arrhythmia using ECG data collected across multiple physical conditions, including sitting, walking, and running. The objective is to evaluate whether Random Forest can maintain high classification performance under varying physiological states, thereby providing a more realistic and generalizable diagnostic framework.

Furthermore, this research emphasizes the role of robust signal preprocessing in improving classification outcomes. By integrating preprocessing, feature extraction, and Random Forest classification into a low-cost, portable, and web-based system, the study aims to support early arrhythmia detection in practical settings. This approach is particularly intended for deployment in underserved or remote regions with limited access to specialized diagnostics. Especially country like Indonesia with many small developing villages, offering an accessible tool to improve patient care.

MATERIALS AND METHODS

This study was conducted at one of the Vocational High Schools in Medan in collaboration with Universitas Padjadjaran Bandung. A total of 26 male students aged 17 to 20 years voluntarily participated in the study. Participants were included based on their willingness to participate, absence of prior cardiovascular disease, and ability to provide informed consent. Students with a history of chronic illness or those undergoing treatment for heart-related conditions were excluded. Prior to data collection, all participants were informed about the objectives and procedures of the study, and written informed consent was obtained. Ethical approval was secured before the commencement of the study to ensure compliance with institutional and ethical research standards.

Nonetheless, the relatively small and homogeneous sample, consisting solely of male participants within a narrow age range, constituted a limitation of the study. Future research was recommended to involve a larger and more diverse population in terms of gender, age, and health status to enhance the external validity and generalizability of the findings. The tools used included an ECG, AD8232, ESP32, an SD card, a Raspberry Pi, Bluetooth, and Wi-Fi, which were selected for their cost-effectiveness, portability, and compatibility with real-time ECG signal acquisition and processing. ECG signals and heart rate patterns were recorded to identify potential arrhythmias across different physical activity levels. Each participant performed sitting, walking, and running tasks for three minutes each.

To capture the signal, the AD8232 module was utilized. The AD8232 received weak analog signals from the body, filtered noise, and amplified them for accurate reading by the microcontroller. After amplification, the ESP32 microcontroller, which featured Bluetooth and Wi-Fi connectivity, captured the amplified signals through its analog-to-digital converter (ADC) input for further digital processing. The converted digital data was then transmitted to the Raspberry Pi, which served as the primary processing unit. The Raspberry Pi managed data storage, display, and subsequent processing and analysis of the incoming ECG signal. The processed data was stored on an SD card for local backup and could be accessed through the ESP32 or directly via the Raspberry Pi. For reliable data transmission, the system supported both Wi-Fi and physical data-cable connections, ensuring flexibility and stability across deployment scenarios. Through Wi-Fi, the Raspberry Pi was also capable of sending the data to a web server for real-time remote monitoring. This integrated setup provided a compact, efficient, and reliable system for continuous heart-rate monitoring.

ECG signals were often affected by various types of noise, including motion artifacts, muscle activity (EMG), and environmental interference. To suppress these components while preserving diagnostic morphology, the raw signals were preprocessed using a fourth-order Butterworth band-pass filter with cutoff frequencies of 0.5 Hz and 40 Hz. This passband retained the P wave (0.5–10 Hz), the QRS complex (10–40 Hz), and the T wave (1–7 Hz), while attenuating baseline wander and high-frequency noise. The Butterworth design was selected because it provided a maximally flat frequency response within the passband, minimizing amplitude distortion and maintaining waveform fidelity. Its smooth response

characteristics made it highly effective for preserving clinically relevant ECG features during noise reduction and signal conditioning.

After filtering, the R peaks of the ECG waveform were automatically detected using the Pan–Tompkins algorithm, a widely recognized method for reliable real-time QRS detection. The algorithm operated through a sequence of processes, including signal differentiation to highlight rapid transitions, squaring to amplify significant changes and ensure positive values, moving-window integration to represent the energy of the QRS complex, and adaptive thresholding to accurately identify R-peak positions. This algorithm was selected because it provided an optimal balance between detection accuracy and computational efficiency, maintaining robust performance even under noisy or motion-affected conditions, which made it suitable for real-time and portable ECG systems. Once R peaks were detected, RR intervals were obtained from consecutive R peaks, and heart rate (HR) was computed in beats per minute as:

$$HR = \frac{60}{RR\ (s)} \qquad (1)$$

Following R-peak detection, additional fiducial points were extracted to enable the computation of key ECG intervals. The Q point was determined by identifying the first local minimum to the left of each R peak, while the S point was located as the next minimum to the right. The onset of the P wave was identified within 150–250 milliseconds before the R peak by detecting the earliest upward deflection and slope change. The T wave was detected within 150–400 milliseconds after the S point using a combination of amplitude thresholding and morphological pattern matching. In cases where the T wave was indistinct, wavelet-based smoothing was applied to improve the accuracy of endpoint detection.

Once all fiducial points were established, temporal intervals were calculated using their relative positions. The PR interval was measured from the onset of the P wave to the beginning of the QRS complex (Q point), the QRS duration (QS interval) was measured from the Q to the S point, and the QT interval was calculated from the Q point to the end of the T wave. The ST segment was determined from the S point to the onset of the T wave. Additionally, the corrected QT interval (QTc) was calculated using Bazett's formula to account for variations in heart rate:

$$QTc = \frac{QT}{\sqrt{RR(s)}} \qquad (2)$$

All extracted features were compiled into a structured dataset consisting of seven predictor variables. The detailed outcomes of the feature extraction process for each subject are presented in Table 1, which provides the interval measurements and derived parameters obtained from the ECG signals.

Table 1. Result of Feature Extraction by Subject

Subject	RR	PR	QS	QT	ST	Heart rate	QTc
S1	731.83	137.72	65.72	398.06	203.01	95.29	508.25
S2	649.30	114.55	72.26	352.39	167.54	106.27	472.99
S3	653.04	144.60	59.99	290.38	196.91	98.62	364.61
S4	551.25	124.42	61.46	244.25	159.54	116.05	329.92
S5	521.42	123.19	65.81	294.40	152.74	117.83	413.10
S6	580.22	133.50	58.17	354.58	172.56	107.42	483.74
S7	560.94	121.74	65.05	304.53	154.63	116.50	425.93
S8	618.17	123.53	71.52	320.79	170.52	100.68	415.96
S9	640.41	130.42	61.88	290.57	180.23	101.12	369.54
S10	531.64	117.94	76.83	391.08	159.96	116.11	538.48
S11	540.89	125.50	59.55	246.69	154.82	114.54	338.33
S12	672.95	141.93	64.07	304.22	175.27	94.86	380.21
S13	549.25	119.87	84.91	285.80	138.58	118.58	399.37
S14	599.44	127.77	67.17	247.01	151.78	104.05	322.28
S15	666.25	132.65	66.83	269.52	171.63	94.50	335.66
S16	538.60	128.10	72.86	290.72	130.82	115.67	404.27
S17	498.70	105.17	66.16	267.96	159.14	123.25	383.16
S18	580.06	118.32	72.60	242.86	157.68	108.39	326.24
S19	576.52	108.41	70.39	314.25	177.34	106.11	419.50
S20	447.50	102.39	64.72	440.18	129.33	137.97	678.67
S21	483.54	107.48	55.88	207.21	92.27	126.66	302.28
S22	524.50	102.57	70.88	255.98	140.11	115.52	354.81
S23	581.44	114.16	60.82	263.75	169.58	104.42	347.22
S24	497.40	105.54	57.59	202.91	108.85	123.58	289.05
S25	531.94	116.30	72.15	319.65	151.95	116.14	445.77
S26	457.18	97.33	79.61	336.76	106.88	132.36	503.85

Source: (Research Results, 2025)

In addition, the overall distribution of the dataset across the five arrhythmia-risk categories
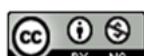
was summarized in Table 2, providing a comprehensive overview of how the subjects were classified based on the extracted features. In this study, a total of 26 subjects participated, each contributed three ECG recordings, resulting in a total of 78 recordings.

Table 2. Class Distribution Table

No.	Value	Range	Total
1	High potential arrhythmia	2099.66 - 2317.53	6
2	Moderately potential arrhythmia	1881.79 - 2099.65	13
3	Potential arrhythmia	1663.92 - 1881.78	26
4	Normal	1446.04 - 1663.91	28
5	Abnormal	1228.16 - 1446.03	5

Source: (Research Results, 2025)

The classification task was performed using a supervised learning approach with the Random Forest algorithm. This ensemble method combined multiple decision trees trained on different subsets of the dataset via bootstrap sampling (bagging). In this study, the model was constructed with 30 decision trees, a number that was chosen to provide sufficient diversity among learners while maintaining computational efficiency. At each decision node, all available predictors were evaluated to determine the optimal split, which allowed the model to fully explore the feature space. The trees were allowed to grow without predefined depth limits and continued splitting until terminal nodes were reached in accordance with node-purity criteria. A 5-fold cross-validation strategy was employed during model development to ensure robustness and reduce the risk of overfitting. The final prediction $\hat{y}$ for an input instance x was obtained through majority voting across all trees in the ensemble. Mathematically, this is defined as:

$$\hat{y} = mode\{h_1(x), h_2(x), \ldots, h_T(x)\} \quad (3)$$

Where $h_t(x)$ represented the predicted class label produced by the t-th decision tree in the ensemble, and T denoted the total number of trees in the Random Forest. The final prediction $\hat{y}$ was determined by taking the mode, or the most frequently predicted class label, among all individual tree outputs. In this study, the classifier was designed to categorize ECG signals into five predefined classes: normal, abnormal, potential arrhythmia, moderately potential arrhythmia, and high potential arrhythmia. To assess the generalization performance of the model, five-fold cross-validation was employed. The dataset was

randomly partitioned into five equal subsets. In each fold, four subsets were used for training and one for validation, such that each subset served as the validation set exactly once. This iterative process helped ensure robust and unbiased performance evaluation. A comprehensive overview of the entire signal processing and classification pipeline was presented in the system block diagram shown in Figure 1.
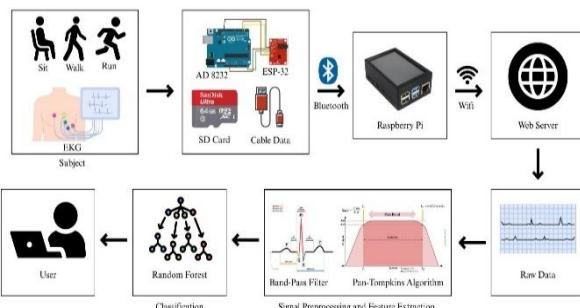
Source: (Research Results, 2025)
**Figure 1.** Block Diagram

RESULTS AND DISCUSSION

To support classification and pattern recognition of ECG signals, a set of physiological parameters was derived from each subject's recording. These features capture individual cardiac activity characteristics and reflect variations influenced by heart condition and physical activity levels. Figure 2 illustrates the variations in ECG interval features, categorized according to three types of physical activity: walking (blue), sitting (orange), and running (gray). Figure 2(a) presents the RR interval, defined as the duration between two consecutive heartbeats measured in milliseconds (ms). As expected, the RR interval is significantly shorter during running compared to walking or sitting, reflecting an increased heart rate associated with more intense physical exertion. In Figure 2(b), the PR interval, representing the conduction time from the onset of atrial activation (P wave) to ventricular activation (start of QRS complex), shows a slightly prolonged duration during sitting. This phenomenon is physiologically attributable to heightened parasympathetic activity in resting conditions, which reduces the conduction speed through the atrioventricular node to optimize cardiac efficiency.

Figure 2(c) depicts the QS interval, corresponding to ventricular depolarization from the onset of the Q wave to the end of the S wave. The QS interval remains relatively stable across all three activities, typically ranging from 0.06 to 0.10 seconds, suggesting a consistent conduction

velocity within the ventricles regardless of heart rate variations. In Figure 2(d), the QT interval which measures ventricular depolarization and repolarization from the start of the QRS complex to the end of the T wave is observed. The QT interval decreases during running, aligning with physiological adaptations where faster heart rates lead to accelerated ventricular repolarization and thus a shortened QT interval.

Lastly, Figure 2(e) presents the ST segment, defined as the period from the end of the QRS complex to the beginning of the T wave, representing the early phase of ventricular repolarization. The graph indicates a reduction in ST amplitude during running activities compared to resting states. This lowering of the ST segment can be attributed to increased myocardial oxygen demand during rapid heart rates, shortened diastolic intervals, and positional shifts of the heart during vigorous movement, potentially causing subtle ischemic effects or altered electrical activity patterns observable in the ECG waveform. Classification within these graphs was performed using a threshold-based method, where ECG intervals were grouped based on predefined.

a)   b)

c)   d)

e)
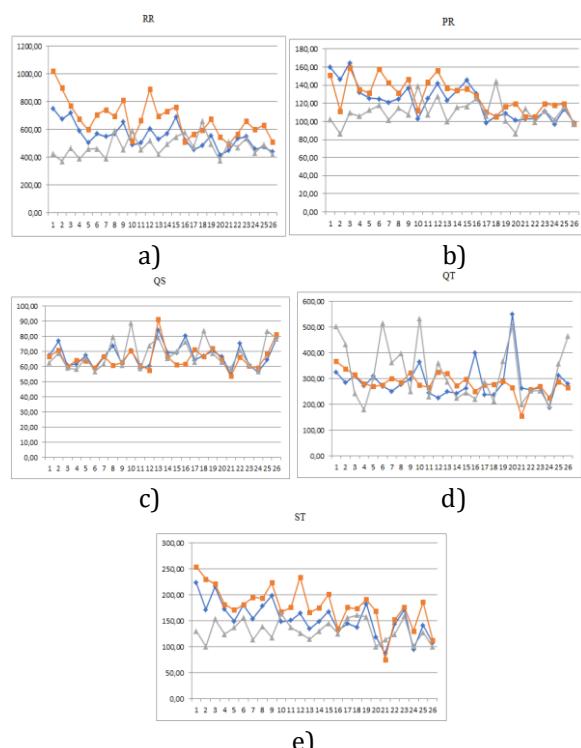
Source: (Research Results, 2025)
Figure 2. Recorded a) RR b) PR c) QS d) QT e) ST wave graph with walking (blue). sitting (orange), and running (gray) colors.

A scatter plot is an effective visualization tool that displays the distribution of observations based on two selected variables. Each point represents one instance, with the x-axis and y-axis corresponding to distinct ECG feature values. In Figure 3, the data points are color-coded to represent five classification categories: abnormal (blue), normal (purple), potential arrhythmia (red), moderately potential arrhythmia (orange), and highly potential arrhythmia (green).

Figure 3(a) illustrates the relationship between the RR and PR intervals. A general positive trend is observed, indicating that an increase in the RR interval tends to be followed by an increase in the PR interval. This trend aligns with physiological expectations, as a slower heart rate (longer RR) may correspond with longer atrioventricular conduction time (PR). Normal category predictions (purple) are clustered within a physiologically plausible range. In contrast, instances classified as potential arrhythmia (red) and highly potential arrhythmia (green) appear when either or both intervals deviate from the normal range.

Figure 3(b) presents the relationship between the PR and QS intervals. The plot reveals clear separation between categories, where normal recordings typically fall within moderate PR and QS interval ranges. Abnormal data points (blue) are concentrated in regions with low PR and QS intervals. High-risk predictions (green) appear in cases where one interval is significantly elevated while the other is reduced, suggesting an irregular conduction pattern. Meanwhile, moderate deviations (orange and red) occur in borderline ranges or under unstable interval conditions.

Figure 3(c) explores the relationship between the QT and QS intervals. Unlike the previous plots, the distribution here does not follow a clear linear pattern. Instead, dispersion is observed across the classification groups. Prolonged QT intervals are associated with the high-risk category (green), while abnormally short intervals are often classified as abnormal (blue). This visualization further supports the capability of the classification model in identifying arrhythmogenic risks based on multivariable relationships between ECG features.


a)

b)

c)
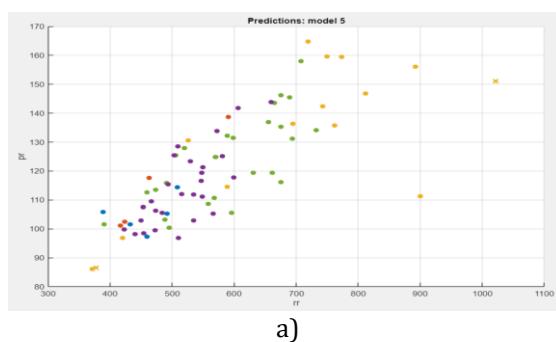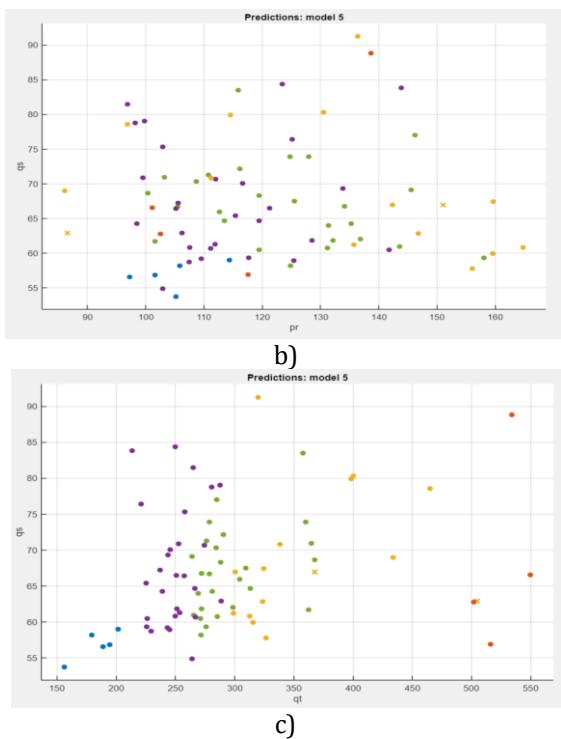
Source: (Research Results, 2025)
Figure 3. Scatter Plot a) RR-PR b) PR-QS c) QT-QS.

In this study, the Confusion Matrix was used to evaluate the performance of the classification model. This matrix presents classification outcomes in terms of four categories: true positive (TP), true negative (TN), false positive (FP), and false negative (FN). A true positive occurs when the model correctly classifies data belonging to a target class, while a true negative represents correct classification of non-target data. Conversely, false positives occur when data are incorrectly predicted as positive, and false negatives arise when positive instances are misclassified as negative. In the graphical representation, correctly classified instances are shown in blue, while misclassifications appear in red, enabling quick visual assessment of model accuracy.

Figure 4(a) presents the classification counts and corresponding observations for each category. The results show that the model accurately predicted four out of five classes: abnormal, normal, potential arrhythmia, and moderately potential arrhythmia. However, two samples of high potential arrhythmia were misclassified as moderately potential arrhythmia, contributing to the false negative rate for that class.

Figure 4(b) highlights the true positive rate (TPR) and false negative rate (FNR). For the high potential arrhythmia category, the TPR reached 66.7%, with the remaining 33.3% falling under the FNR due to misclassification. All other categories

abnormal, normal, potential arrhythmia, and moderately potential arrhythmia achieved a perfect TPR of 100%. Figure 4(c) presents the positive predictive value (PPV) and false discovery rate (FDR). The PPV for the abnormal, normal, potential arrhythmia, and high potential arrhythmia classes was 100%, indicating all predicted instances were correctly classified. The moderately potential arrhythmia class showed a PPV of 86.7%, with an FDR of 13.3%, suggesting some overlap with nearby risk categories. These evaluation metrics underscore the effectiveness of the model while also identifying areas for potential refinement.

a)

b)

c)
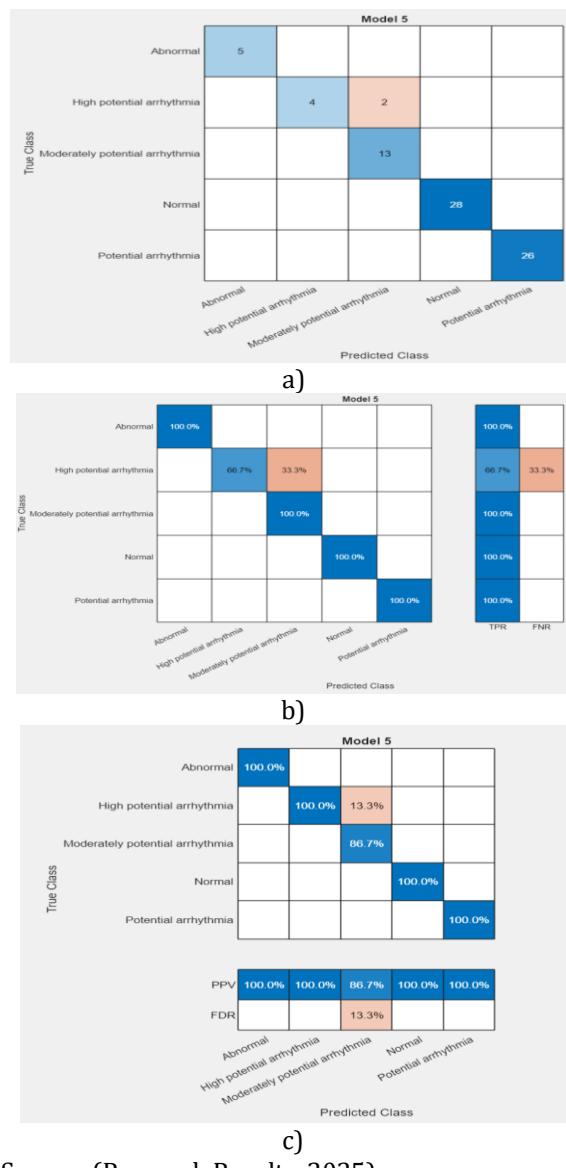
Source: (Research Results, 2025)
Figure 4. a) Number of Observations b) True Positive Rate (TPR) and False Negative Rate (FNR) c) Positive Predictive Value (PPV) and False Discovery Rate (FDR).

Beyond visual interpretation, the confusion matrix also forms the basis for calculating key performance metrics such as accuracy, precision (positive predictive value), recall (true positive rate), and F1-score which each formula is explained in Equations (4) to (7)

$$Accuracy = \frac{TP+TN}{TP+TN+FP+FN} \quad (4)$$

$$Precision = \frac{TP}{TP+FP} \quad (5)$$

$$Recall = \frac{TP}{TP+FN} \quad (6)$$

$$F1 - Score = 2 \times \frac{Precision \times Recall}{Precision+Recall} \quad (7)$$

After applying Random Forest, the next step is to evaluate the performance of the resulting models. The assessment is carried out using evaluation metrics such as accuracy, precision, recall and F1-score to discover the effectiveness of the algorithms in making predictions on the processed data. Besides that, it can also be used to identify prediction errors in the model, which is shown in Table 3.

Table 3. Model Evaluation Results

No.	Class	Accuracy	Precision	Recall	F1-Score
1	Abnormal	97%	100%	100%	100%
2	High potential arrhythmia	97%	100%	67%	80%
3	Moderately potential arrhythmia	97%	100%	100%	100%
4	Normal	97%	100%	100%	100%
5	Potential arrhythmia	97%	93%	100%	96%
	Average	97%	98%	98%	98%

Source: (Research Results, 2025)

The Receiver Operating Characteristic (ROC) curve in Figure 5 illustrates the trade-off between the true positive rate (TPR) and false positive rate (FPR) for each classification category. The area under the curve (AUC) serves as a key metric in evaluating the classifier's ability to distinguish between classes. The model achieved a perfect AUC score of 1.0 for the abnormal, normal, and potential arrhythmia categories, indicating excellent sensitivity and specificity with no misclassification. The moderately potential arrhythmia category also performed well, with an AUC of 0.984, suggesting high reliability and strong class separability. In contrast, the high potential

arrhythmia category yielded a lower AUC of 0.8819. While still acceptable, this result indicates reduced classification precision relative to other categories. Two possible factors may explain this outcome. First, the limited number of training samples for this class could have restricted the model's learning ability. Second, the extracted features for high potential arrhythmia may substantially overlap with those of the moderately potential category, complicating accurate differentiation.

To improve classification in this category, two strategies are recommended. Increasing the number of representative training samples would help balance the dataset and improve learning generalization. In addition, incorporating more discriminative features such as frequency-domain parameters, refined morphological characteristics, or nonlinear heart rate variability measures could enhance the model's ability to distinguish subtle differences specific to high-risk arrhythmia. Visually, the ROC curves for the abnormal, normal, and potential arrhythmia categories cluster near the upper-left corner, confirming strong performance in these classes. A slight deviation is observed in the moderately potential arrhythmia curve, while a more noticeable deviation appears in the high potential arrhythmia category. Despite this, the ROC analysis demonstrates the robustness of the classification model across four out of five categories, while highlighting the need for further refinement in high-risk arrhythmia detection.
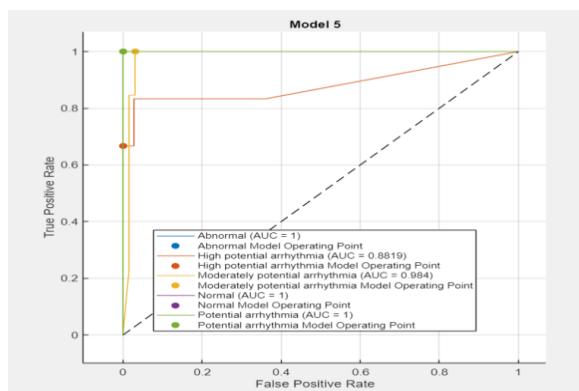
Source: (Research Results, 2025)
Figure 5. ROC Curve Validation

CONCLUSION

This study successfully demonstrated the classification of ECG signals into five arrhythmia risk categories: normal, abnormal, potential arrhythmia, moderately potential arrhythmia, and high potential arrhythmia through signal preprocessing, feature extraction, and the Random Forest algorithm. The developed model achieved a

high accuracy of 97.4%, confirming its effectiveness and robustness in distinguishing cardiac risk patterns. These results suggest the feasibility of a low-cost, compact, and automated ECG analysis system that could support early arrhythmia screening in resource-limited settings where access to trained cardiologists is constrained.

Nevertheless, important limitations should be acknowledged. The study was conducted with a relatively small and homogeneous cohort of young, healthy participants, limiting generalizability to broader clinical populations. Furthermore, the current feature set relied solely on time-domain intervals, which may not fully capture the complex morphology and frequency characteristics of pathological ECGs. Misclassifications were most evident in the high-potential arrhythmia category, attributable to both the small sample size and the feature overlap with adjacent risk groups.

Future research should therefore focus on more representative datasets that include diverse age groups and confirmed clinical diagnoses, along with external validation across independent cohorts. Incorporating more discriminative features, such as frequency-domain indices, advanced morphological descriptors, and nonlinear heart rate variability measures, together with class-balancing strategies could enhance performance, particularly in high-risk categories. Attention should also be given to deployment challenges, including real-world noise, variability across devices, regulatory requirements, and interpretability for clinical end-users. Clinically, features such as PR, QRS duration, and QTc are established indicators of conduction abnormalities and arrhythmia risk, reinforcing the potential of the proposed model as a complementary screening tool in early cardiac risk assessment.

REFERENCES

[1]   S. Manao D. Sitanggang A. Sagala A. Oktarino and M. Turnip "Journal of Computer Networks Architecture and High Performance Computing APPLICATION OF KNN METHOD FOR CLASSIFICATION OF ARRHYTHMIA TYPES BASED ON ECG DATA Journal of Computer Networks Architecture and High Performance Computing vol. 7 no. 3 pp. 629–637 2025.

[2]   D. Farell *et al* "Classification of Arrhythmia Potential using the K-Nearest Neighbor Algorithm *Internetworking Indones. J* vol. 16 no. 2 pp. 3–9 2024.

[3]   M. P. Rivaldi "Overview of Heart and Vascular Disease Patients at Lamaddukelleng Sengkang Hospital in 2023 *An Idea Heal. J* vol. 5 no. 02 pp. 151–157 2025.

[4]   N. E. Almansouri *et al.*, "Early Diagnosis of Cardiovascular Diseases in the Era of Artificial Intelligence: An In-Depth Review," *Cureus*, vol. 16, no. 3, pp. 1–18, 2024, doi: 10.7759/cureus.55869.

[5]   M. Turnip I. Putra D. Telaumbanua A. Nicol A. Dharma and D. Sitanggang "Early Identification of Potential Heart Abnormalities with Decision Tree Method *Proc. - 2024 2nd Int. Conf. Technol. Innov. Its Appl. ICTIIA 2024* 2024 doi: 10.1109/ICTIIA61827.2024.10761420.

[6]   P. Kamga R. Mostafa and S. Zafar "The Use of Wearable ECG Devices in the Clinical Setting: a Review *Curr. Emerg. Hosp. Med. Rep* vol. 10 no. 3 pp. 67–72 2022 doi: 10.1007/s40138-022-00248-x.

[7]   C. Spaccarotella A. Polimeni C. Mancuso G. Pelaia G. Esposito and C. Indolfi "Assessment of Non-Invasive Measurements of Oxygen Saturation and Heart Rate with an Apple Smartwatch: Comparison with a Standard Pulse Oximeter *J. Clin. Med* vol. 11 no. 6 pp. 0–6 2022 doi: 10.3390/jcm11061467.

[8]   A. Emmett B. Kent A. James and J. March-McDonald "Experiences of health professionals towards using mobile electrocardiogram (ECG) technology: A qualitative systematic review *J. Clin. Nurs* vol. 32 no. 13–14 pp. 3205–3218 2023 doi: 10.1111/jocn.16434.

[9]   S. Bala *et al* "Comparative study on the quality of electrocardiogram and arrhythmia detection using wireless ambulatory Vigo SmartHeart Holter and conventional Holter *MRIMS J. Heal. Sci* vol. 12 no. 3 pp. 166–170 2024 doi: 10.4103/mjhs.mjhs_148_22.

[10]   P. C. Chang M. S. Wen C. C. Chou C. C. Wang and K. C. Hung "Atrial fibrillation detection using ambulatory smartwatch photoplethysmography and validation with simultaneous holter recording *Am. Heart J* vol. 247 pp. 55–62 2022 doi: 10.1016/j.ahj.2022.02.002.

[11]   A. A. Hamidi B. Robertson and J. Ilow "A new approach for ECG artifact detection using fine-KNN classification and wavelet scattering features in vital health applications *Procedia Comput. Sci* vol. 224 pp. 60–67 2023 doi: 10.1016/j.procs.2023.09.011.

[12]   Z. Li and H. Zhang "Fusing deep metric

learning with KNN for 12-lead multi-labelled ECG classification *Biomed. Signal Process. Control* vol. 85 no. February p. 104849 2023 doi: 10.1016/j.bspc.2023.104849.

[13] H. Yadav *et al* "CNN and Bidirectional GRU-Based Heartbeat Sound Classification Architecture for Elderly People *Mathematics* vol. 11 no. 6 pp. 1–25 2023 doi: 10.3390/math11061365.

[14] R. R. Van De Leur *et al* "Discovering and Visualizing Disease-Specific Electrocardiogram Features Using Deep Learning: Proof-of-Concept in Phospholamban Gene Mutation Carriers *Circ. Arrhythmia Electrophysiol* vol. 14 no. 2 p. E009056 2021 doi: 10.1161/CIRCEP.120.009056.

[15] N. Jannah S. Hadjiloucas and J. Al-Malki "Arrhythmia detection using multi-lead ECG spectra and Complex Support Vector Machine Classifiers *Procedia Comput. Sci* vol. 194 pp. 69–79 2021 doi: 10.1016/j.procs.2021.10.060.

[16] K. Sharma and R. K. Sunkaria "Cardiac arrhythmia detection using cross-sample entropy measure based on short and long RR interval series *J. Arrhythmia* vol. 39 no. 3 pp. 412–421 2023 doi: 10.1002/joa3.12839.

[17] M. Badr S. Al-Otaibi N. Alturki and T. Abir "Detection of Heart Arrhythmia on Electrocardiogram using Artificial Neural Networks *Comput. Intell. Neurosci* vol. 2022 2022 doi: 10.1155/2022/1094830.

[18] B. Krithiga P. Sabari I. Jayasri and I. Anjali "Early detection of coronary heart disease by using naive bayes algorithm *J. Phys. Conf. Ser* vol. 1717 no. 1 2021 doi: 10.1088/1742-6596/1717/1/012040.

[19] D. Setiawan Ali Muhammad and Siti Herawati Fransiska Dewi "Penerapan Algoritma Klasifikasi untuk Deteksi Dini Penyakit Jantung Koroner Berdasarkan Gejala Klinis *Tek. J. Ilmu Tek. dan Inform* vol. 5 no. 1 pp. 18–26 2025 doi: 10.51903/teknik.v5i1.706.

[20] J. N. Sari P. Madona H. Kusryanto M. M. Zain and M. Valzon "Electrocardiogram signals classification using random forest method for web-based smart healthcare *Int. J. Adv. Appl. Sci* vol. 12 no. 2 pp. 133–143 2023 doi: 10.11591/ijaas.v12.i2.pp133-143.

[21] Q. Mastoi H. Farman and S. Ahmed "Novel framework for Efficient Detection of QRS Morphology for The Cardiac Arrhythmia Classification | Journal of Computing & Biomedical Informatics vol. 05 no. 02 2023 [Online]. Available: https://jcbi.org/index.php/Main/article/view/190

[22] A. Masbakhah, U. Sa'adah, and M. Muslikh, "Heart Disease Classification Using Random Forest and Fox Algorithm as Hyperparameter Tuning," *J. Electron. Electromed. Eng. Med. Informatics*, vol. 7, no. 4, pp. 964–976, 2025, doi: 10.35882/jeeemi.v7i4.932.